

Study of a Power Generation System for Distributed Power Supplies that Utilizes the High-Pressure Dissociation Characteristics and the Small Difference in the Temperature of CO₂ Hydrate*

Shin'ya OBARA**, Manabu OKUDA**, Ryouhei SHIMIZU**, Masahito KAWAI*** and Kazuhiro MATSUMURA****

**Power Engineering Laboratory, Department of Electrical and Electronic Engineering, Kitami Institute of Technology
Koen-cho 165, Kitami, Hokkaido 090-8507, Japan
E-mail: obara@mail.kitami-it.ac.jp

***Support Center for Engineering Education, Hakodate National College of Technology
Tokura-cho 14-1, Hakodate, Hokkaido 042-8501, Japan

****Department of Research and Development, Hokkaido Industrial Technology Center
Kikyo-cho 379, Hakodate Hokkaido 041-0801, Japan

Abstract

When the mixed fluid of gas and water is pressurized and cooled to a given pressure and temperature, the generation of a gas-hydrate occurs. By heating, a very high pressure is obtained from the dissociated gas from the gas-hydrate. The purpose of this study is to investigate the operation of a high-pressure gas engine generator for distributed power supplies using the high pressure obtained through the dissociation of a gas-hydrate. A gas-hydrate functions as a working fluid and as a form of energy storage. However, until now, an actuator that uses the dissociation inflation characteristics of a gas-hydrate has not been examined. Therefore, the generation rate of CO₂ hydrate and the quantity to be stored from the dissociation expansion energy of CO₂ hydrate were investigated. As a result, when 1 m³ of water was used to generate CO₂ hydrate for 480 minutes, the result was that electric power corresponding to approximately 45% of the daily power consumption (4.5 kWh of generator outputs) of an individual house can be stored.

Key words: CO₂ Hydrate, Energy Storage, Power Generation, Distributed Power System, High-Pressure Gas Engine, Low-Temperature Exhaust Utilization

1. Introduction

The pressure-temperature characteristics of a gas-hydrate include a large differential pressure that is obtained from a small difference in temperature. Therefore, a clean power generation system could potentially be constructed by using the low-temperature exhaust heat of a factory, the difference in temperature between day and night, the green energy created by the hydrate generation cycle. A gas-hydrate holds a gas molecule with a clathrate compound.

The generation rate of a gas-hydrate is influenced by the solubility of the gas. When generating a hydrate using a gas with a high solubility in water, it is thought that a clathrate is formed after the gas fully dissolves in water. The pressure-temperature characteristics of the gas-hydrate change greatly with the types of gas¹⁾. For example, in the case of CO₂ hydrate, a pressure differential (difference in the highest pressure of the gas dissociation and the minimum pressure of the hydrate generation) of approximately 3 MPa can be obtained on the phase equilibrium curve of generation and dissociation for an approximately 10 °C difference in temperature. Moreover, when the temperature of a methane hydrate is changed from 0 °C to 10 °C, a pressure differential of 4 MPa or more will occur on the phase equilibrium curve. Therefore, we were examining the operation of a high-pressure gas engine generator according to the differential pressure obtained from the difference in temperature and the gas-hydrate. In this paper, the basic technology of an engine generator operated by a high-pressure gas for distributed power supplies is investigated. Until now, gas hydrates have been examined in many fields, such as the transportation of fuel gas and the undersea storage of CO₂²⁻⁴⁾. However, the application of CO₂ hydrate in the working fluid of an actuator has not yet been studied.

Production of the gas-hydrate by green energy and exhaust heat means clean energy storage. However, the energy density of the energy storage, the energy storage velocity, the energy release velocity, etc., of CO₂ hydrate has not been fully investigated. Therefore, in this paper, the generation rate of CO₂ hydrate and the quantity of the dissociation expansion energy to be stored are clarified by tests and numerical analysis.

2. Characteristics of CO₂ Hydrate and Application to a Distributed Power Supply

Figure 1 is a phase diagram of CO₂ hydrate¹⁾. Generally, the difference in the minimum pressure of the generation time and the highest pressure at the time of gas dissociation of the gas-hydrate can be obtained for a narrow temperature change. For example, when CO₂ hydrate at 0 °C is heated to 10 °C, a differential pressure of approximately 3 MPa can be obtained, as shown in Fig. 1. A high-pressure gas engine generator can be operated using this differential pressure. Cold and warm states can be created from green energy, such as the difference in temperature between the day and the night, low temperature exhaust heat, the sunlight, and wind power generation in a cold region. When an engine generator using the expansion characteristics of the dissociation of CO₂ hydrate proposed in this study (CH engine generator) is realized, a new, clean, distributed power generation system can be constructed. Furthermore, although CO₂ hydrate can provide energy storage, because the generation rate of the hydrate is slow, it is expected that the energy density of a CH engine

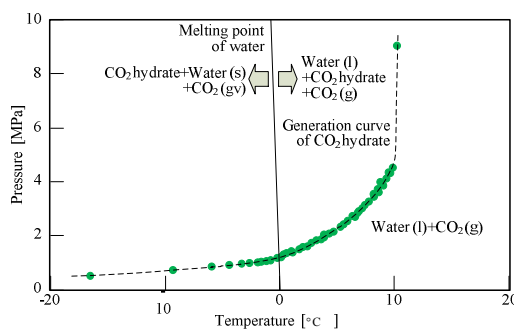


Fig. 1 Phase diagram of CO₂ hydrate

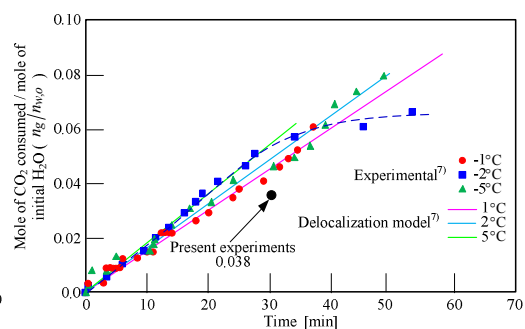


Fig. 2 Experimental and analytic results in the early period of CO₂ hydrate growth

generator will be low. Until now, because there are no examples of using CO₂ hydrate as the working fluid of an actuator, the possibility of the practical use of a CH engine generator is not known. In this paper, the generation rate of CO₂ hydrate and the quantity of the dissociation expansion energy of the hydrate to be stored are investigated, and the energy density of a CH engine generator is clarified.

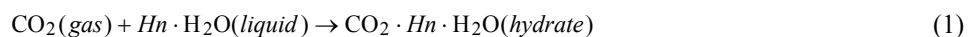
3. Numerical Analysis

3.1 Generation of CO₂ Hydrate

The dissolved amount of CO₂ in water is large, and the amount of CO₂ contained in 100 cm³ of water at 25 °C and 100 kPa is 0.145 g. For these conditions, the value of the consumed CO₂ in moles divided by the moles of water ($n_g/n_{w,o}$) in Fig. 2 is 0.000593 (described later). The amount of CO₂ hydrate grows by keeping CO₂ fully dissolved in water under the generation condition of a hydrate. Moreover, it is known from many hydrate generation experiments that a gas-hydrate has a memory effect⁵⁾. The generating time is short when the water is used in the generation and the dissociation of the hydrate is maintained under the generation conditions of the hydrate. The physical phenomenon described above is called the memory effect of a hydrate. It is thought that the memory effect occurs because the next nucleation becomes easier through the survival of part of the hydrate structure in the liquid water phase⁶⁾. Moreover, it was reported by Kawamura et al. in 2002 that the generation rate of CO₂ hydrate at an icy melting point can be compared with the generation rate at other temperature and pressure conditions⁷⁾. Fig. 2 shows the results of the experiments and the analysis of the generation rate of CO₂ hydrate at an icy melting point reported by Kawamura et al.

3.2 Generation Rate of CO₂ Hydrate

The following equations are the generation reaction equation of CO₂ hydrate.



Here, Hn is a theoretical hydration number and $Hn=5.75$ for a filling factor of 1. However, the filling factor is normally 7 to 8⁸⁻¹³⁾. Moreover, the specific gravity of CO₂ hydrate is 1.1, which is greater than seawater^{14, 15)}.

The Englezos-Bishnoi model¹⁶⁾ is introduced into the calculation of the growth rate of a hydrate¹⁷⁾. The fugacity difference is assumed to be the driving force in the Englezos-Bishnoi model. Equation (2) is a computation expression for the CO₂ gas volume consumed with the growth of the hydrate. $n_g(t)$ is proportional to the amount of water (the number of moles), $n_w(t)$, in the container, and the gas-liquid contact area is proportional to amount of water, as assumed in Eq. (2).

$$\frac{dn_g(t)}{dt} = K' \cdot (f_{ex} - f_{eq}) \cdot n_w(t) = K' \cdot (f_{ex} - f_{eq}) \cdot \{ n_{w,o} - Hn \cdot n_g(t) \} \quad (2)$$

Fugacity is defined as the pressure of an ideal gas with the same chemical potential as a certain real gas. Here, when it is assumed that $K' \cdot (f_{ex} - f_{eq})$ and Hn are constant, the following formula can be obtained by integrating the above equation.

$$\frac{n_g}{n_{w,o}} = \frac{1}{H_n} \cdot [1 - \exp\{-H_n \cdot K' \cdot (f_{ex} - f_{eq}) \cdot t\}] \quad (3)$$

Although the generation process of a hydrate is investigated here, as shown in Eq. (4), it is necessary to adjust Eq. (3) for the amount of CO₂ dissolved before the hydrate is generated.

$$\frac{n_g}{n_{w,o}} = \frac{1}{hn} [1 - \exp\{-hn \cdot K' \cdot (f_{ex} - f_{eq}) \cdot t\}] + \frac{n_{gf}}{n_{w,o}} \quad (4)$$

Here, n_{gf} is the number of moles of CO₂ dissolved in water and hn is the hydration number at the time of generation of the hydrate obtained from the following equation:

$$hn = \frac{1}{(q_1 - q_2) \cdot n_{w,o}} \quad (5)$$

Here, q_1 is the number of moles of CO₂ contained in 1 mol of water after hydrate completion, and q_2 is the number of moles of CO₂ included in 1 mol of water at the time of generation. The hydration number, H_n , is 8.13, which is confirmed by the experiment of Haneda et al.¹³⁾. Although hn is 11, it differs based on the conditions.

3.3 External Work of a High-Pressure Fluid

(1) CO₂ gas

The computation expression of the heat insulation work shown in Eq. (6) is introduced into the energy conversion of the gas expansion by an actuator.

$$P_{CO_2} \cdot V_{CO_2}^\kappa = \text{constant} \quad (6)$$

Here, P_{CO_2} , V_{CO_2} , and κ are the pressure of the CO₂ gas, the volume, and the ratio of the specific heat, respectively. When the CO₂ gas arrives at the exit (condition (P_b, V_b)) from the inlet port (condition (P_a, V_a)) of an actuator, the gas is assumed to be experiencing adiabatic expansion. In this case, the CO₂ gas at P_a and T_a works adiabatically to P_b . The temperature in the actuator exit of the CO₂ gas is calculated from the following equation:

$$T_b = T_a \cdot \left(\frac{P_b}{P_a}\right)^{(\kappa-1)/\kappa} \quad (7)$$

The work, L_{CO_2} , obtained by the expansion of the CO₂ gas is determined using the following equation, where R_{CO_2} is a gas constant of CO₂:

$$L_{CO_2} = G_{CO_2} \cdot \frac{R_{CO_2}}{\kappa-1} \cdot (T_a - T_b) \quad (8)$$

The work (L_{vp}) of the steam, as well as the calculation method described above, is obtained.

(2) Liquid water

The high-pressure water under the conditions (P_a , T_a) can be used to calculate the work, L_{H_2O} , at the time the conditions change to (P_b , T_b) by the following equation:

$$L_w = V_w \cdot \Delta P_{a-b} \tag{9}$$

Here, V_w is a mass flow rate of water and ΔP_{a-b} is the pressure differential of the operating points a and b.

The work, L_{chd} , obtained from the pressure increase of each gas and the water from the dissociation of CO₂ hydrate in an enclosed space is a combination of Eqs. (8) and (9), where L_{vp} on the right-hand side of Eq. (10) is the heat insulation work done by the steam.

$$L_{chp} = L_{CO_2} + L_{vp} + L_w \tag{10}$$

The mechanical efficiency of the actuator, except for the generator, and the efficiency of the generator are set to η_a and η_e , respectively. The power output, W , from the actuator (engine generator) is calculable by the following equation:

$$W = L_{chp} \cdot \eta_a \cdot \eta_e \tag{11}$$

3.4 Heating Value of Dissociation and Generation of CO₂ Hydrate

The latent heat, h_{ch} , of CO₂ hydrate is approximately 500 kJ/kg¹⁸⁾. The heat of dissociation, $H_{d,t}$, and the heat of formation, $H_{re,t}$, of CO₂ hydrate during a sampling time, t , are obtained from the following equations, respectively. Here, ΔT_{d-ost} is the difference in temperature between the dissociation temperature of CO₂ hydrate and the outside air temperature, and ΔT_{ost-r} is the difference in the outside air temperature and the generation temperature of CO₂ hydrate. The calculation of the heating value in Eqs. (12) and (13) is based on the outside air temperature.

$$\begin{aligned} H_{d,t} &= (H_{w,s,t} + H_{CO_2,s,t}) \cdot \Delta T_{d-ost} + H_{ch,l,t} \\ &= (G_w \cdot h_{w,s} + G_{CO_2} \cdot h_{CO_2}) \cdot \Delta T_{d-ost} + G_{CO_2} \cdot h_{ch} \end{aligned} \tag{12}$$

$$\begin{aligned} H_{r,t} &= (H_{w,s,t} + H_{CO_2,s,t}) \cdot \Delta T_{ost-r} + H_{ch,l,t} \\ &= (G_w \cdot h_{w,s} + G_{CO_2} \cdot h_{CO_2}) \cdot \Delta T_{ost-r} + G_{CO_2} \cdot h_{ch} \end{aligned} \tag{13}$$

4. Generation and Dissociation Experiments of CO₂ Hydrate

4.1 Experimental Device

Figure 3 shows the outline of an experimental device used for the investigation of the dissociation and the generation of CO₂ hydrate. As shown in Fig. 3 (a), this experiment device consists of double pipe heat exchangers and supplied a heat-exchanger fluid for cooling and heating the inner pipe. The space between the outside pipe and the inner pipe was filled with pure water and CO₂ (this space is described as an examination space below). The volume of this examination space was approximately 100 cm³. The outside diameter and bore of the outside pipe were 25.4 mm and 21.2 mm, and the outside diameter and bore of the inner pipe were 12.8 mm and 10.2 mm. Moreover, the outside pipe shown in Fig. 3 (a) was approximately 450 mm in length. As shown in Fig. 3 (b), N₂ for the replacement of

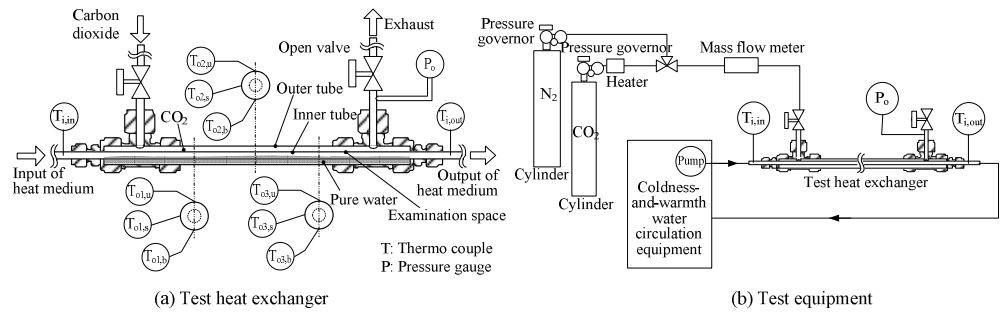


Fig. 3 Generation and dissociation test equipment of CO₂ hydrate

the examination space could be supplied to the experimental device. A temperature sensor (T-type covering thermocouple) was installed in the outer wall of the outside pipe, and was used to measure the input/output of the heating medium. The pressure in the examination space was measured using a pressure sensor (Fig. (a)). Because the pressure in the examination space was 3 MPa or more, the temperatures of the water, the CO₂, and the CO₂ gas-hydrate in the examination space were not measured directly in this experiment.

4.2 Experimental Method

Because the solubility of CO₂ is large, the test equipment filled up with CO₂ is placed 30 minutes or more. The pressure of the examination space before each test is adjusted to 3 MPa. The examination space was filled with CO₂ and 50 cm³ of pure water. Furthermore, an improvement in the generation speed of the hydrate as the result of the memory effect was expected, and the generation and dissociation steps were repeated several times in the experiment. Moreover, the heat of generation and dissociation of CO₂ hydrate was fully supplied in this experiment.

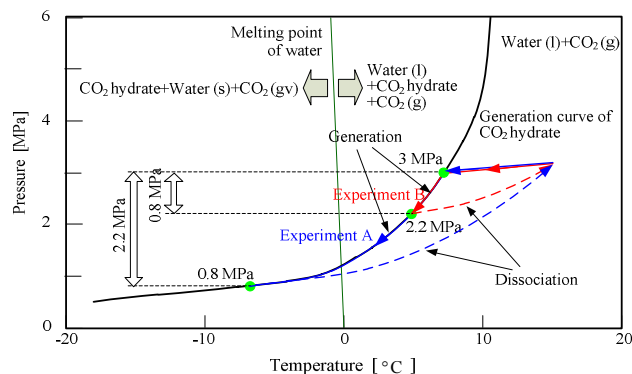


Fig. 4 Generation process of CO₂ hydrate

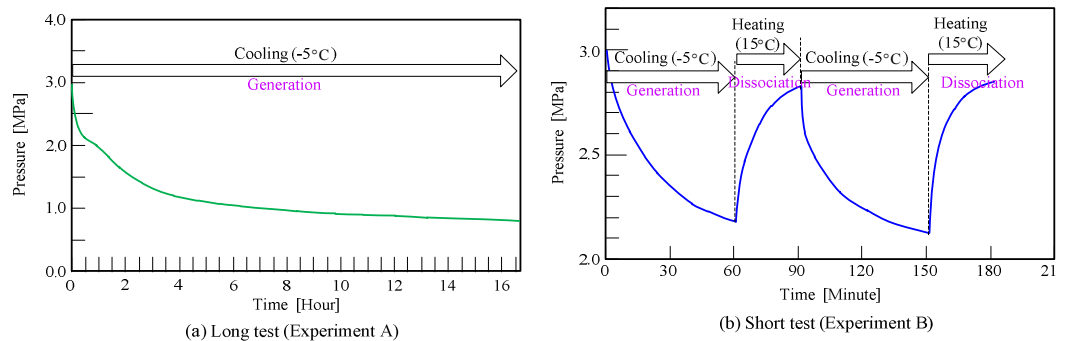


Fig. 5 Experimental results of the pressure of CO₂ dissolution test

5. Results and Discussion

5.1 Generation Process of CO₂ Hydrate

Figure 4 shows the expected change of state in the long generation experiment of CO₂ hydrate (Experiment A) and the experiment with the repeated generation and dissociation steps (Experiment B). The examination space is fulfilled with CO₂ and pure water (respectively about 15 °C). Next, a cold medium was supplied to the inner pipe, and the fluid in the examination space was cooled. As a result and as shown in Fig. 4, it was expected that the temperature and the pressure would decline along the generation curve for CO₂ hydrate.

5.2 Generation Rate of CO₂ Hydrate

Figures 5 (a) and (b) are the experimental results of Experiment A and B, respectively. The heat-exchanger fluid temperature at the time of the hydrate generation in each experiment was -5 °C. Moreover, the heat-exchanger fluid temperature in the dissociation step in Experiment B was 15 °C. The generation of CO₂ hydrate was continued in Experiment A for 16 hours or more. In contrast, the generation of CO₂ hydrate for 1 hour and the dissociation for 30 minutes were repeated in Experiment B. As shown in Fig. 5(a), we found that if the test time exceeded 4 hours, the generation speed of CO₂ hydrate would decrease. Moreover, the generation rate for the first 30 minutes was the lowest compared with the other time zones. The generation time of CO₂ hydrate was 1 hour in Experiment B. Compared with the generation time of CO₂ hydrate, the speed of the gas dissociation was low. The gas dissociation of Experiment B was approximately 30 minutes. In the equation for the state of an ideal gas, the pressure drops by contraction upon gaseous cooling. Therefore, to clarify the difference between the decreased pressure accompanying the generation of CO₂ hydrate and the decreased pressure caused by contraction of CO₂, N₂ was used instead of CO₂. This result is shown in Fig. 6, where heat was automatically radiated after cooling for 1 hour. When N₂ was cooled, a decrease in pressure of approximately 0.2 MPa was seen at the maximum in Fig. 6. Therefore, the decreased pressure from the cooling of CO₂ was contained in the generation of CO₂ hydrate shown in Fig. 5.

Based on the experimental results of Experiment A and B, the amount of CO₂ consumption accompanying the generation of the CO₂ hydrate is plotted in Fig. 2. The results of this experiment were lower than each result of reference⁷⁾. This is because each result of reference⁷⁾ was a value at an icy melting point because the generation rate of the hydrate was obtained very early in the process. Furthermore, the generation speed of a hydrate easily changes as the result of factors such as the structure and the churning state of the test equipment and the heat transmission in the examination space.

5.3 Generation Characteristics of CO₂ Hydrate

(1) Energy storage time

Although CO₂ hydrate can be used an operational fluid in a power generation system, CO₂ hydrate also has an energy storage function. That is, the energy from the pressure increase at the time of gas dissociation can be stored during the generation of CO₂ hydrate. Therefore, in this paper, the amount of energy stored and the storage time for CO₂ hydrate were investigated. Figure 7 shows the experimental results of the differences in pressure (difference between the highest pressure at the time of gas dissociation and the minimum

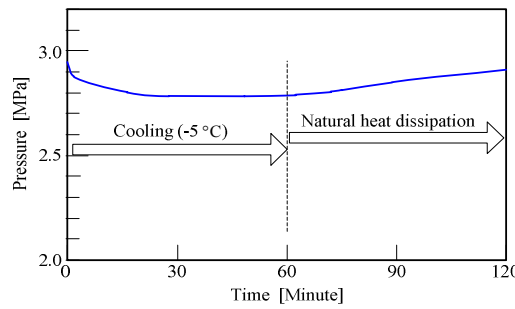


Fig. 6 Results of the reference test using N₂

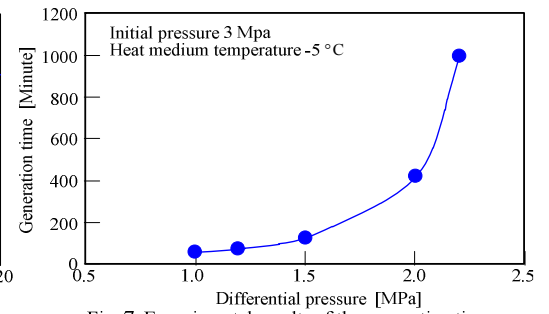


Fig. 7 Experimental results of the generation time for obtaining a pressure differential

pressure at the time of hydrate generation) and the CO₂ hydrate generation time obtained at the initial pressure of 3 MPa and a heat-exchanger fluid temperature of -5 °C. This result changes significantly with the setting of the heat-exchanger fluid temperature. In the result shown in Fig. 7, if the pressure difference is greater than 1.5 MPa, the generation time of the hydrate will rapidly become greater.

(2) The relationship between the temperature and the pressure difference of CO₂ hydrate

Figure 8 shows the difference in the highest pressure at the time of gas dissociation of CO₂ hydrate and the minimum pressure at the time of CO₂ hydrate generation (in this case, 15 °C and 6 MPa). For example, if CO₂ hydrate can be cooled to -10 °C, the differential pressure will be approximately 5 MPa. If the generation temperature of CO₂ hydrate is low, a large pressure difference can be obtained, as seen in Fig. 8, but at approximately 0 °C or less, the change in the pressure difference is small. It is thought that CO₂ hydrate continues to be generated at 0 °C or lower, although there is almost no increase in the pressure difference. Below 0 °C, it is surmised that the concentration ratio of CO₂ hydrate to water increases.

5.4 Energy Storage Amount

(1) Generation rate of CO₂ hydrate

Figure 9 shows the results of the consumption of CO₂ during generation of hydrates. The experimental results, with an initial pressure of 3 MPa (red curve) and the analytical result with an initial pressure of 6 MPa calculated using Eq. (4) are shown in the figure. The difference in the experimental results and the analytical results with an initial pressure of 3 MPa after 120 minutes is large. Furthermore, the characteristic of the experimental result after 20 minute differs greatly even from the beginning of the experiment. The difference between the experimental result after 120 minutes and the analytical result allows us to conclude that the dissolution of CO₂ in water was not high enough and that the heat exchange experienced an unsmooth phase change in the double-tube heat exchanger. Ice and CO₂ hydrate are formed on the outside of the inner tube early in the experiment, and the heat conduction with a quick rate of heat transfer is dominant in the growth of the hydrate. However, the resistance to heat transfer may increase because the thickness of the hydrate layer increases with time. It is necessary to further examine the cause of the difference between the experimental value after 120 minutes and the analytic value.

(2) Energy storage time

Figure 10 shows the experimental result and the analytical results of the generating time and the energy storage velocity when CO₂ hydrate is generated in 1 m³ of water. The initial

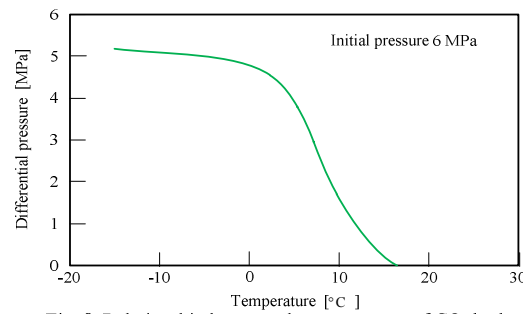


Fig. 8 Relationship between the temperature of CO₂ hydrate and the differential pressure

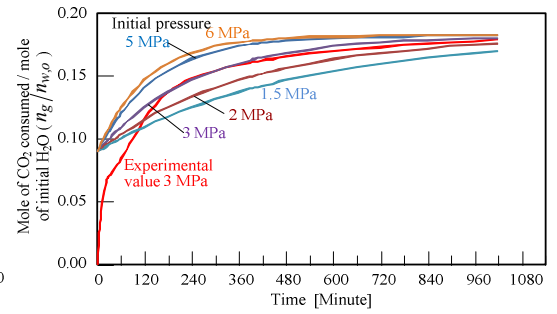


Fig. 9 Generation characteristics of CO₂ hydrate

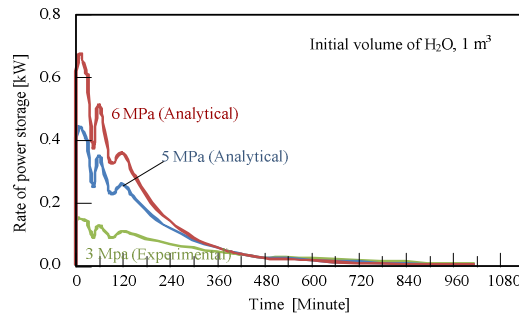


Fig. 10 Analytical results of the rate of power storage

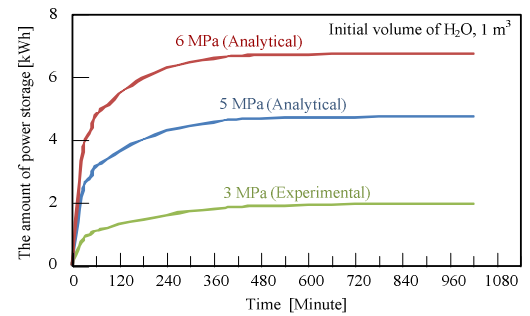


Fig. 11 Analytical results of the amount of power storage

pressure of 3 MPa in the figure is an experimental result, and the results with an initial pressure of 5 and 6 MPa were obtained from the numerical analysis. The analytical result was obtained by calculating the generated amount of CO₂ hydrate from $n_g/n_{w,o}$, as shown in Fig. 9, and then calculating Eq. (9) from Eq. (7) to obtain the storage pressure assumed from the above value. Finally, Eq. (10) was calculated, where K' in Eq. (4) is set equal to the value obtained from the experimental results for every sampling time and an initial pressure 3 MPa. For this reason, the fluctuation after 120 minutes that was observed in the experiment with an initial pressure of 3 MPa also appeared in the analytical results for initial pressures of 5 and 6 MPa. The energy storage velocity from the generation of CO₂ hydrate is the same regardless of the initial pressure after more than 360 minutes.

Figure 11 shows the ratio of the energy storage amount of CO₂ hydrate to 1 m³ of water. An initial pressure of 3 MPa is an experimental result, and the pressures of 5 and 6 MPa in Fig. 11 are analytic results. Most increases in the energy storage amount are not seen after approximately 480 minutes, as shown in Fig. 11. The daily power consumption from an individual house, excluding the cooling and the heating load, is approximately 10 kWh. The energy storage capacity of a CH engine generator with an initial pressure of 6 MPa is approximately 45% of this value (4.5 kWh of generating end outputs). This result was used to calculate η_a and η_e from Eq. (11) as 0.8 and 0.85, respectively.

6. Conclusions

An actuator is operated by observing the differential pressure obtained from a given difference in temperature and CO₂ hydrate. This study aimed to develop a high-pressure gas engine generator for distributed power supplies. Therefore, in this paper, the generation characteristics of CO₂ hydrate, the generation rate, and the quantity of dissociation expansion energy which is available to be stored were investigated. The following conclusions were reached:

- (1) The differential pressure between the generation and the gas dissociation of CO₂ hydrate increases so that the temperature of the hydrate is low. However, when the temperature of a hydrate is less than 0 °C, the increase in differential pressure will become very small. However, it is thought that the concentration ratio of CO₂ hydrate to water increases.
- (2) The energy storage velocity accompanying the generation of CO₂ hydrate will become almost the same as the initial pressure when the generating time exceeds 360 minutes.
- (3) When 1 m³ of water is made to generate a hydrate for 480 minutes, the electric power corresponding to approximately 45% of the daily power consumption (4.5 kWh of generating end outputs) of an individual house, minus the cooling and heating load, can be stored.

The difference between the experimental result and the analytic result after 120 minutes of CO₂ hydrate generation is large and needs to be clarified.

Nomenclature

- A : gas-liquid contact area [m²/mol]
 f_{eq} : fugacity of the gas in a three-phase equilibrium condition [MPa]
 f_{ex} : fugacity of the gas for the experimental condition [MPa]
 G : mass [kg]
 H : heat [W]
 h : specific heat [kJ/(kg·K)]
 h_{ch} : latent heat of CO₂ hydrate [kJ/kg]
 h_n : the hydration number concerning generation of CO₂ hydrate
 $H_{ch,l}$: the amount of latent heat of CO₂ hydrate [kJ]
 $H_{CO_2,s}$: the amount of sensible heat of CO₂ [kJ]
 H_d : the amount of heat of dissociation of CO₂ hydrate [kJ]
 H_n : theoretical hydration number
 H_r : the amount of heat of formation of CO₂ hydrate [kJ]
 $H_{w,s}$: the amount of sensible heat of CO₂ [kJ]
 K : velocity constant [/(MPa·min·m²)]
 K' : total velocity constant [/(MPa·min)] ($K' = K \cdot A$)
 L : external work [J]
 L_{chd} : work by the pressure increase of gas and water [J]
 n_g : CO₂ gas volume incorporated into the hydrate [mol]
 n_w : amount of water [mol]
 $n_{w,o}$: the number of moles of the initial first water [mol]
 P : pressure [Pa]
 q_1 : the number of moles of CO₂ included in 1 mol of water after hydrate completion [mol]
 q_2 : the number of moles of CO₂ included in 1 mol of water of hydrate generation [mol]
 R_{CO_2} : gas constant of CO₂ [kJ/(kg·K)]
 T : temperature [K]
 t : sampling time [s]
 ΔT_{d-ost} : the difference in temperature between the dissociation temperature and the

- outside air temperature [K]
 ΔT_{ost-r} : the difference in temperature between the outside air temperature and the generation temperature [K]
 V : volume [m³]
 W : power output of generating end [W]

Roman character

- κ : ratio of specific heat

Subscript

- a : entrance of the actuator
 b : exit of the actuator
 ch : CO₂ hydrate
 w : water

Acknowledgments

We received support for this research from the Yazaki Memorial Foundation for Science and Technology 2010. We greatly appreciate the support of this foundation.

References

- (1) D. Sloan, A. C. Koh, Clathrate hydrates of natural gases, CRC Press 2007, New York, USA.
- (2) Pietro Di Profio, Simone Arca, Federico Rossi, Mirko Filippini, Comparison of hydrogen hydrates with existing hydrogen storage technologies: Energetic and economic evaluations, International Journal of Hydrogen Energy, 2009, 34(22), 9173-9180.
- (3) B. Kvamme, A. Graue, T. Buanes, T. Kuznetsova, G. Ersland, Storage of CO₂ in natural gas hydrate reservoirs and the effect of hydrate as an extra sealing in cold aquifers, International Journal of Greenhouse Gas Control, 2007, 1(2), 236-246.
- (4) Geir Ersland, Jarle Husebø, Arne Graue, Bjørn Kvamme, Transport and storage of CO₂ in natural gas hydrate reservoirs, Energy Procedia, 2009, 1(1), 3477-3484.
- (5) W. Shimada, M. Ohshima, Memory effect of TBAB hydrate -the effect of aqueous solution concentration and churning-, No. 21, Proceedings of Japanese Society of Snow and Ice, Hokuetsu branch, 2009. in Japanese.
- (6) R. Ohmura, Y. Mori, Physical chemistry of clathrate hydrates -an overview and a state-of-the-art review of fundamental studies contributing to energy and environmental technology, Thermal Science and engineering, 1999, 7(2), 35-38. in Japanese.
- (7) T. Kawamura, T. Komai, Y. Yamamoto, K. Nagashima, K. Ohgaa, K. Higuchi, Growth kinetics of CO₂ hydrate just below melting point of ice, Journal of Crystal Growth, 2002, 234, 220-226.
- (8) C. Oyama, Experimental study on the generation characteristics of CO₂ hydrate film under deep sea conditions, University of Tsukuba, Graduate School of Systems and Information Engineering, Master thesis, 2004. in Japanese.
- (9) A. K. Sum, R. C. Burrus and E. D. Sloan Jr, Measurement of clathrate hydrates via Raman Spectroscopy, J. Phys. Chem. B., 1997, 101, 7371-7377.
- (10) J. A. Ripmeester and C. I. Ratcliffe, The diverse nature of dodecahedral cages in clathrate hydrates as revealed by ¹²⁹Xe and ¹³C NMR spectroscopy: CO₂ as a small-cage guest, Energy Fuels, 1998, 12, 197-200.
- (11) C. I. Ratcliffe and A. J. Ripmeester, ¹H and ¹³C NMR studies on carbon dioxide hydrate, J. Phys. Chem., 1986, 92, 1259-1263.
- (12) T. Uchida, A. Takagi, J. Kawabata, S. Mae and T. Honda, Raman spectroscopic analysis on the growth process of CO₂ hydrate, Energy Convers. Mgmt, 1995, 36, 547-550.

- (13) H. Haneda, T. Kawamura, T. Komai, Y. Yamamoto, Y. Ogata, K. Ohga, K. Higuchi, Shigen-to-Sozai, 2001, 117, 731-735.
- (14) H. Teng, A. Yamasaki and Y. Shindo, Stability of the hydrate layer formed on the surface of a CO₂ droplet in high-pressure, Low-Temperature, Chem. Eng. Sci., 1996, 51, 4979-4986.
- (15) K. Ohgaki, T. Hamanaka, Phase-Behavior of CO₂ Hydrate-Liquid CO₂-H₂O System at High Pressure, Journal of Chemical Engineering of Japan, 1995, 21(4), 800-803. in Japanese.
- (16) P. Englezos and P. R. Bishnoi, P.R. Prediction of gas hydrate formation conditions in aqueous electrolyte solutions, AIChE Journal, 1988, 34, 1718-1721.
- (17) H. Haneda, T. Kawamura, T. Komai, Y. Yamamoto, K. Aoki, K. Ohga, Fundamental study of artificial loof construction, using carbon dioxide gas in methane hydrate development : growth behavior of CO₂ hydrate in model sediment, Journal of the Mining and Materials Processing Institute of Japan, 2004, 120(3), 159-163. in Japanese.
- (18) Sandrine Marinhas, Anthony Delahaye, Laurence Fournaison, Didier Dalmazzone, Walter Fürst, Jean-Pierre Petit, Modelling of the available latent heat of a CO₂ hydrate slurry in an experimental loop applied to secondary refrigeration, Chemical Engineering and Processing, 2006, 45(3), 184-192.